Anisotropy of the Thermal Conductivity of Stretched Amorphous Polystyrene in Supercritical Carbon Dioxide Studied by Reverse Nonequilibrium Molecular Dynamics Simulations

Elena A. Algaer,* Mohammad Alaghemandi, Michael C. Böhm, and Florian Müller-Plathe

Eduard-Zintl-Institut für Anorganische und Physikalische Chemie, Technische Universität Darmstadt, Petersenstrasse 20, D-64287 Darmstadt, Germany

Received: July 8, 2009; Revised Manuscript Received: September 15, 2009

The thermal conductivity (λ) of stretched amorphous atactic polystyrene (PS) swollen in supercritical carbon dioxide (sc CO_2) has been investigated over a wide temperature, pressure, and concentration range. Nonequilibrium molecular dynamics simulations with a full atomistic force-field have been employed to calculate the thermal conductivity of neat stretched PS and of different mixtures of supercritical CO_2 with stretched PS. As the energy transport in PS parallel and perpendicular to the stretching direction differs, an anisotropy in the thermal conductivity occurs. The magnitude of λ is enhanced with an increasing number of carbon−carbon backbone bonds oriented parallel to the direction of the heat transport. The degrees of freedom in the side chain of the polymer are rather unimportant for the thermal conductivity. To understand the conditions leading either to an equivalence or nonequivalence of the system degrees of freedom for the heat transport, we have analyzed λ of PS, CO_2, binary PS−CO_2 mixtures and other model systems as a function of the bond constraints in the computational model. Furthermore, we have commented on differences in the thermal conductivity provided either by a vibrational energy transfer or by collisions.

1. Introduction

For many years, polymers have already played a crucial role in the development of new products. In connection with silicon based microelectronics, the interest in these systems has grown significantly. Polymers are widely employed both as on-chip dielectric materials and as an active layer in plastic electronic devices.[1,2] These promising facts have led to an increasing industrial interest in polymer materials and their physical properties. The thermal conductivity (λ) plays a central role in a number of processes and applications, such as polymeric thermal insulation, encapsulation of electronic devices, and so on.

Many polymers are highly anisotropic. Properties such as elastic moduli,[3,4] viscosity,[5] and electrical conductivity[6] have been investigated in detail in these materials. The thermal conductivity is one of the quantities where an anisotropic behavior has been studied, too.[7–11] It has been observed in polymers with an amorphous structure as well as in partially oriented samples.[11] Anisotropies in the thermal conductivity have been found both in experimental and in simulation studies.[11,12] In the design of modern polymer-based products, the anisotropy in physical properties should be considered carefully, as it brings new possibilities to the design of novel materials that can be used in electronics, for example. Accurate theoretical predictions of λ and its anisotropy can lead to improvements in the processing and application design. For instance, the thermal conductivity of insulating materials is a determining factor in their energy efficiency.[13] Thermal conductivities of polymers over a wide temperature and pressure range are not always available. In this case, computer simulations of the molecular dynamics (MD) type become an important instrument for the prediction of the thermal conductivity of polymers.[14] The correlation between measured heat capacities and calculated thermal conductivities can be used to derive physically reliable force-field parameters in simulation methods. These techniques finally offer the possibility to relate measured λ values to structural units of polymers.

Another focus of recent polymer studies is swelling processes in supercritical fluids. Much work has been done for mixtures of a polymer and CO_2 under supercritical conditions. The large ecological advantage of CO_2 in comparison to organic solvents is its nontoxicity.[15–17] Furthermore, it has been shown experimentally that the substitution of toxic organic solvents by CO_2 under supercritical conditions does not lead to strong reductions in the yield of purification, impregnation, and fractionation as well as in the production of porous foam or powder polymers.[18,19] To optimize these processes, it is necessary to investigate the physical properties of polymers swollen in supercritical media. Experimental and simulation approaches have been used simultaneously to determine these polymer properties.[20,21] The behavior of many polymers in supercritical fluids is still not understood quantitatively. From the point of view of fundamental science, the investigation of the thermal conductivity of polymers and swollen polymers can lead to the better understanding of the heat transfer process itself. It has been described theoretically that at least two mechanisms are relevant for the heat transport in polymers, that is, vibrational effects and collisions.[22,23] To come back to the anisotropy of the thermal conductivity; this quality has been analyzed in several experimental and theoretical studies on polymers, such as amorphous polystyrene (PS) and polyethylene.[7,11,24]

In this article, we have investigated the anisotropy of the thermal conductivity of stretched atactic polystyrene swollen in supercritical CO_2 by reverse nonequilibrium molecular dynamics (RNEMD) simulations.[14,25–28] The schematic structure of a single PS chain and the arrangement of stretched PS in the

* Corresponding author. E-mail: e.algaer@theo.chemie.tu-darmstadt.de.

10.1021/jp906447a CCC: $40.75
Published on Web 10/09/2009

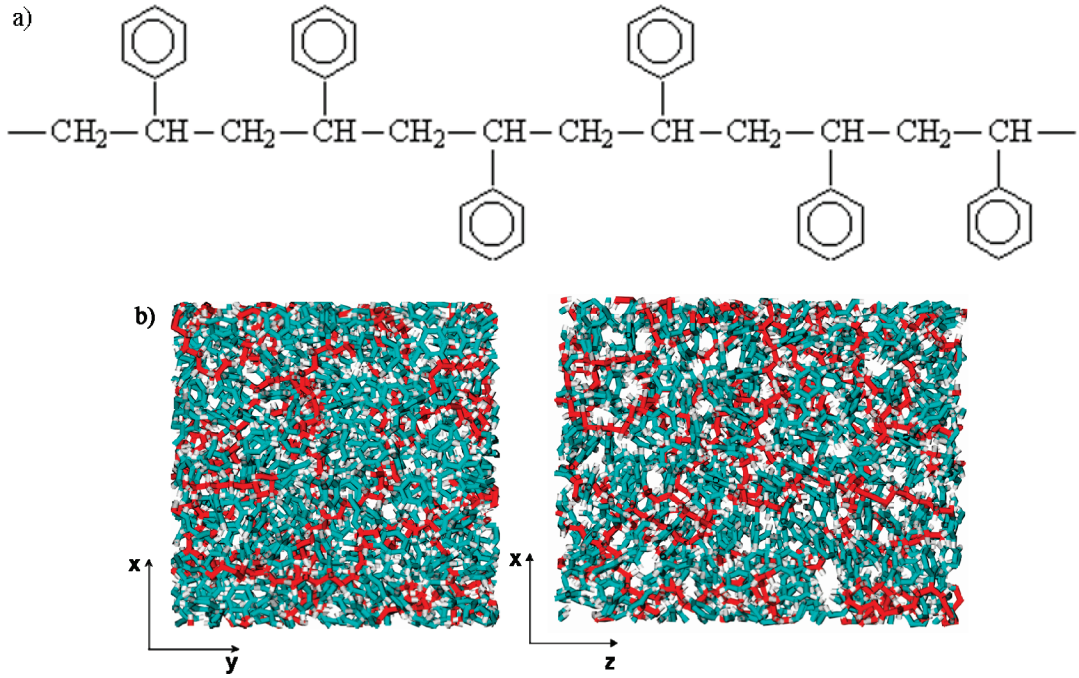

Figure 1. (a) Schematic representation of atactic polystyrene which is characterized by a random distribution of the phenyl rings. (b) Arrangement of stretched polystyrene in the simulation box as projected on the *xy* and *xz* plane. Stretching occurs in the *z* direction. The carbon atoms in the backbone chain have been highlighted in red.

MD simulation box have been displayed in Figure 1. Atactic polystyrene is characterized by a random distribution of the phenyl rings on both sides of the chain; see Figure 1a. The simulation box in the RNEMD approach with a stretched PS chain is presented in Figure 1b. The carbon−carbon bonds of the backbone in Figure 1b are marked in red color. As one can see from the *xz* projection in Figure 1b, the simulation cell is elongated along the *z* direction, while the *x* and *y* dimentions are identical.

In our previous RNEMD study of the thermal conductivity in PS−CO_2 mixtures under supercritical conditions,[28] we have analyzed the implications of finite-size effects and the quasi-degeneracy in multilevel systems.[28,29] In such polymer systems or solids, one can have local changes in the density or in the spatial arrangement of the atoms that are energetically quasi-degenerate but are responsible for anisotropy in physical quantities. In our recent article, we have detected such finite-size effects via anisotropy in the thermal conductivity of PS although we have employed an isotropic simulation cell. An analysis of these computational results has shown that the thermal conductivity strongly correlates with the orientation and number of the C−C bonds in the backbone of PS.[28] This interesting finding has been a strong motivation for the present research. Stretching of the PS sample and the PS−CO_2 mixtures, say into the *z* direction, causes an enhanced orientation of these C−C backbone bonds in this preferred direction. Thus, we expect an enhancement of the thermal conductivity relative to this direction. In other words, in our recent work, any anisotropy has been an outcome of finite-size effects or quasi-degeneracy. Now it has been generated via the sample preparation in the simulation runs.

The thermal conductivity of neat PS and CO_2 as well as of different binary mixtures has been calculated in our previous article and compared with experimental results.[28] The simulation box adopted in these RNEMD simulations has been isotropic. In the present work, we have analyzed the anisotropy of the thermal conductivity in stretched polystyrene. Differences in λ between oriented and unoriented PS samples have been described in the literature many years ago.[7,24] The present study, however, has not been restricted to a comparison with these experimental results but covers general theoretical considerations as well. In recent MD simulations of our group, the thermal conductivity of polyamide-6,6[12] and of the crystalline δ phase of syndiotactic PS[27] has been calculated. In polyamide-6,6, it has been shown that the system degrees of freedom are more or less equivalent; that is, the thermal conductivity strongly correlates with their number. Crystalline PS, however, is a polymer system, where this equivalence is violated. In analogy to ref 28, the decisive influence of the orientation of the C−C backbone bonds relative to the direction of the temperature gradient on λ has been pointed out in ref 12. This comparison with recent theoretical results forms the second main topic of the work at hand. To sum up, in polymers, we can find systems where all degrees of freedom have an identical influence on λ, and we can also have systems where certain degrees of freedom play a dominant role. This contribution aims to find out which concept applies to amorphous polystyrene.

2. Computational Details

As the nonequilibrium technique adopted has been described in recent articles of the group, we refer the reader to these references.[14,25,26] The molecular dynamics simulations in the present article have been performed with the YASP package,[30,31] which makes use of the leapfrog algorithm and orthorhombic periodic boundary conditions. The chosen temperatures and pressure ranges refer to conditions close to experiment. The intramolecular force-field is defined by harmonic bond stretching, harmonic angle bending, and periodic cosine-type torsional potentials. This diagonal approximation attenuates coupling effects between the different degrees of freedom that are decisive for anharmonicity on the potential energy surface. In a number of theoretical studies,[32–35] it has been demonstrated that such anharmonic effects might lead to an enhancement of the thermal

conductivity or to thermal rectification as a response to a polarization of the vibrational energy. The implications of such polarization effects have been analyzed by the present authors in a recent study.[36] We wish to point out that the diagonal force-field adopted is sufficient for the topic discussed below. The nonbonded potential in the present simulations is described via Lennard-Jones terms with Lorentz−Berthelot mixing rules[37] for unlike interactions and via electrostatic interactions that are mapped by atomic partial charges. The electrostatic field has been computed by the reaction-field method with a relative permittivity of 2.5. A cutoff of 1.1 nm has been used in all simulations. A detailed description of the force-field can be found in ref 38. The nonbonded interactions were evaluated from a Verlet neighbor list, which was updated every 15 timesteps (of 0.001 ps length) using a link-cell method with a cutoff of 1.2 nm.

The molecular dynamics simulations have been performed at constant (overall) temperature and pressure. A coupling time τ_T of 0.2 ps has been used for the Berendsen thermostat,[39] while the coupling time τ_P for the Berendsen barostat amounts to 2 ps. Both parameters have been sufficient to keep the calculated average temperature within 1 K of the target temperature and the calculated average pressure within 1 kPa of the target pressure. It has been checked that modifications of τ_T and τ_P did not change the thermal conductivity. The simulation box in the RNEMD runs has been divided into 20 slabs in the heat flux direction. The velocities of the atoms of identical mass were exchanged every 0.5 ps. We have controlled that the thermal conductivity converges within this exchange period. A non-equilibrium run typically covered 3 ns; the last 1 ns has been used for the production.

One atactic polystyrene chain of 300 monomers and random tacticity has been generated in vacuum. The initial conformations have been obtained via pivot Monte Carlo calculations[40] of a single polymer chain in vacuum with a bond-based interaction cutoff to generate a melt-like structure. Since the persistence length is the length over which correlations in the tangential direction are lost, an interaction cutoff of 7 bonds $\approx$ 0.895 nm (persistence length of PS) has been chosen. This chain has been inserted into the periodic simulation cell of a cubic box. The initial density of PS has been 0.908 g/cm^3. Simulations with a soft-core potential have been employed to remove possible overlaps, entanglements and concatenations. Then, the system has been equilibrated for 10 ns by equilibrium MD at a constant pressure of 101.3 kPa and a temperature of 300 K. Equilibration yielded a cubic simulation box with a PS density of 1.042 g/cm^3, while experimental values vary in the range from 1.032 g/cm^3 to 1.069 g/cm^3 at the same conditions.[41]

In the subsequent steps 1 to 5, the simulation box has been stretched. The strategy used has been tested before.[12] (1) Heat the sample over 400 ps at constant volume to 600 K. Use a coupling time of 0.1 ps for the thermostat and a heating rate of 0.5 K/ps. (2) Equilibrate the sample at 600 K for 200 ps at constant volume. (3) Stretch the sample in a NPT simulation of 100 ps duration using a temperature coupling time of 0.1 ps. Note that the pressure coupling is anisotropic. The initial target pressure of 100 000 kPa refers to the average pressure of step 2. The coupling times for the x, y, z directions amount to 150, 150, and 1 ps. The target pressure has been kept constant for the x and y directions. For the z direction, it has been reduced by −600 kPa/ps leading to an enlargement in the z dimension of the box. In our simulations, the sample has been stretched up to 10−25% to simulate changes in the thermal conductivity as a function of the stretching ratio. As practically no contraction was allowed in the x and y directions, the density of the sample has been lower than the density of the isotropic sample at the end of this step. (4) Cool the sample to 400 K in a NPT simulation of 200 ps. The initial bath temperature of 600 K has been lowered with a rate of −0.5 K/ps, and the target pressure has been fixed to 60 000 kPa in all directions. At the end of this step, the density of 1.02 g/cm^3 is still lower than the density of the isotropic sample. (5) Now perform an isotropic compression of the sample in a NPT simulation at 400 K with a target pressure of 60 000 kPa. This step generates a density of 1.04 g/cm^3. Subsequently, the sample has been equilibrated in different NPT simulations (at temperatures in the range between 300 and 500 K, pressures of 0.1 kPa, and 8, 16, 40, and 60 MPa). Now the densities of the stretched samples have achieved the densities of isotropic samples.[28]

A flexible full atomistic model has been selected for the present MD approach. The force constants for PS have been reported previously for a rigid bond model.[38] The constants for the harmonic bond stretching forces have been adopted from other works.[12,42] Potential parameters and atomic charges for a flexible full atomistic model of carbon dioxide have been developed by Harris and Yung[43] with the aim to reproduce its vapor−liquid coexistence curve and critical properties. This setup has been used also for the determination of transport properties such as the self-diffusion coefficient in a supercritical state. The capability of the Harris−Yung model for transport properties, such as a thermal diffusion coefficient, has been discussed in the literature.[44] In analogy to our recent study,[28] we have used these force constants without further modifications.

The following systems have been investigated: neat PS, neat CO_2 at supercritical conditions, and mixtures of PS with different concentrations of CO_2 at supercritical conditions. The simulations have been performed in a temperature range between 350 and 500 K and for pressures between 101.3 kPa and 60 MPa. Both the temperature and the pressure ranges considered have been employed in experimental studies of the mixture.[17,45] They include the investigation of the solubility of PS in supercritical CO_2 and the miscibility of the two components. Studies of the thermal conductivity, however, are not available. The concentration of carbon dioxide in the mixture spans a range from 10 to 30 mass %. Four different mixtures with a total number of 79, 125, 177, and 304 CO_2 molecules added to a single PS chain have been studied. The binary systems generated contain 10, 15, 20, and 30 mass % of CO_2.

3. Results and Discussion

3.1. Thermal Conductivity of Neat Stretched Polystyrene. One of the purposes of the present work has been the investigation of the mechanism of the heat transport. Our hypothesis is that the heat transport in polymers through delocalized phonons[22,23] is more efficient than the transport via collisions. This can lead to the situation that the orientation of certain bonds is of great importance for the heat transfer. Contrary to polymer systems the main heat transport channel in amorphous structures such as CO_2 or benzene is provided by collisions. Our hypothesis will be discussed in detail under consideration of recent findings.

In our previous work, we have calculated the thermal conductivity of neat isotropic polystyrene and compared our data with experimental results.[28] The measured thermal conductivity of neat PS at 300 K and 101.3 kPa amounts to 0.156 W m^{1-} K^{-1}, while the calculated value is of 0.187 W m^{1-} K^{-1}. Possible reasons for this difference have been mentioned already in our recent article.[28] Now we relate the thermal conductivity

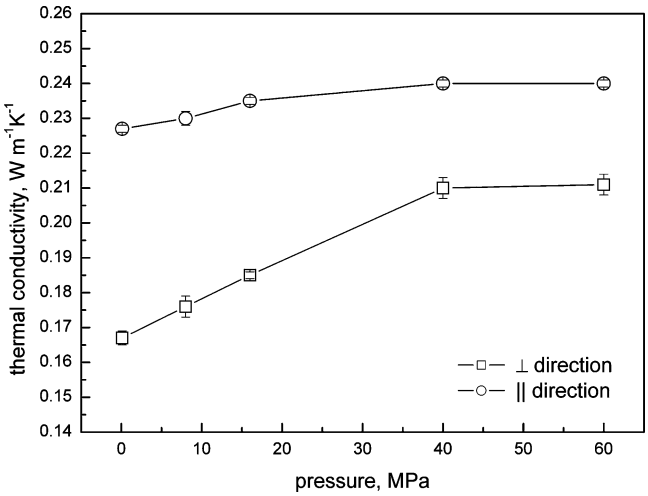

Figure 2. Pressure dependence of the thermal conductivity of anisotropic polystyrene at 400 K and a stretching ratio of 35%.

of anisotropic polystyrene to λ of the isotropic system. The stretched polystyrene sample is characterized by the stretching ratio r_s

$$r_s = \frac{L_{\parallel} - L_{\perp}}{L_{\parallel}} \cdot 100 \qquad (2)$$

where $L_{\parallel}$ and $L_{\perp}$ stand for the length of the simulation box parallel and perpendicular to the stretching direction.

The pressure dependence of the thermal conductivity of the anisotropic polystyrene sample at 400 K and a stretching ratio of 35% is presented in Figure 2. An anisotropy in λ exists at all pressures. The difference between the thermal conductivity parallel $\lambda_{\parallel}$ and that perpendicular $\lambda_{\perp}$ to the stretching direction, however, decreases with increasing pressure. In the parallel direction, the sample behaves as a rather incompressible solid, which is characterized by a weak pressure dependence of the thermal conductivity. The pressure dependence of $\lambda_{\perp}$ is stronger. Here, the limit of an incompressible solid is approached only for pressures larger than 40 MPa. The difference between $\lambda_{\parallel}$ and $\lambda_{\perp}$ can be traced back to different densities in the covalent PS backbone bonds in the two directions. The larger number of covalent backbone bonds in the parallel direction makes the solid both less compressible and better conductive, while the nonbonded contacts in the perpendicular direction allow a compression of the solid over a larger pressure range. The same effect has been observed in graphite with its highly anisotropic compressibility;[46] the planar Young modulus of graphite is roughly 30 times higher than that in the *c* axis direction.

The temperature dependence of the thermal conductivity of anisotropic polystyrene at 100 kPa and a stretching ratio of 21% is shown in Figure 3. To allow a comparison with the isotropic PS data, we have added these values to the diagram. As already reported in our recent study,[28] the thermal conductivity of isotropic PS first increases with temperature, it has a plateau in the range between 400 and 450 K, and then it is slightly reduced; see also Figure 3. From the figure, we deduce the same trend for the anisotropic sample in both directions. The splitting between the two thermal conductivity curves in anisotropic PS does not depend on the temperature.

On the basis of the material in Figure 2, it can be assumed that the difference between the thermal conductivity in the parallel and perpendicular direction is enhanced with an

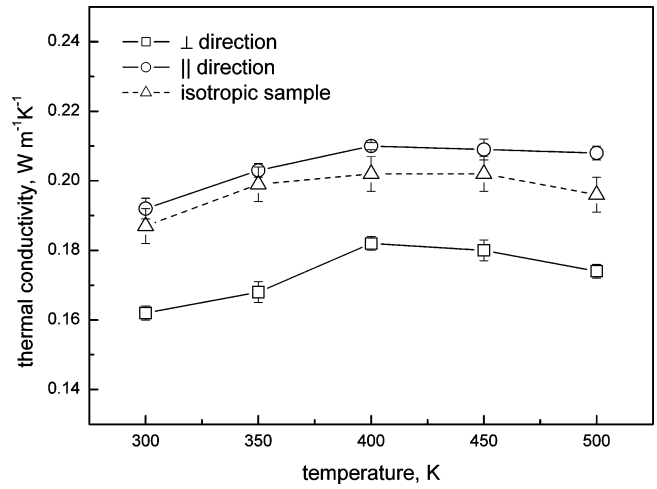

Figure 3. Temperature dependence of the thermal conductivity of anisotropic polystyrene at 100 kPa and a stretching ratio of 21%. The isotropic PS data (dashed curve) have been taken from ref 28.

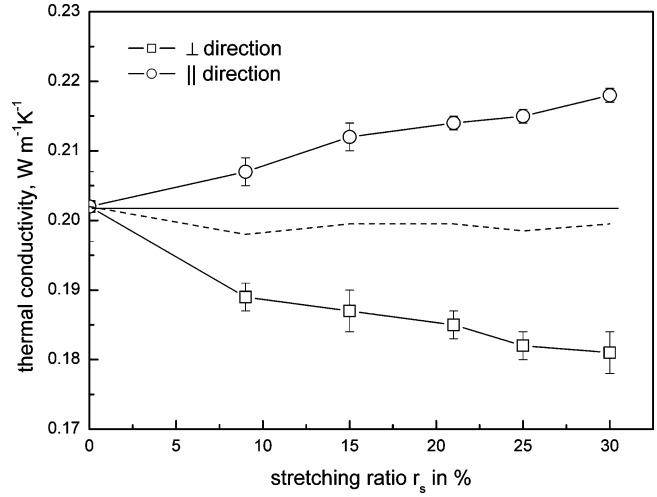

Figure 4. Thermal conductivity of anisotropic polystyrene as a function of the stretching ratio r_s at 100 kPa and 400 K. The average of the $\lambda_{\parallel}$ and $\lambda_{\perp}$ curves has been labeled by a dashed curve. The straight line refers to the thermal conductivity of the isotropic sample; it has been taken from ref 28. This straight line has been given as a guide for the eye.

increasing stretching ratio r_s. A computational verification of this behavior would be an additional support of our hypothesis, that is, the correlation between the orientation of C−C backbone bonds and the magnitude of λ. The thermal conductivity of anisotropic samples as a function of r_s is plotted in Figure 4; it shows the expected behavior. Also note that the average of the two λ curves is slightly smaller than λ of the isotropic sample which has been added for comparison. Figure 4 visualizes that the conductivity reduction in the stretched sample is constant over a large r_s range.

In the following, let us consider the correlation between the number and the orientation of the C−C backbone bonds of PS relative to the direction of the heat transfer and the thermal conductivity in more detail. The distribution function of the direction cosine of these bonds parallel to the direction of the stretching is shown in Figure 5. The distribution is calculated from the PS trajectory with a stretching ratio of 15%, a temperature of 350 K, and a pressure of 101.3 kPa. It has been averaged over 1000 frames, which corresponds to a simulation time of 1 ns. The negative cosine values in the distribution have been inverted and added to the positive ones. One immediately

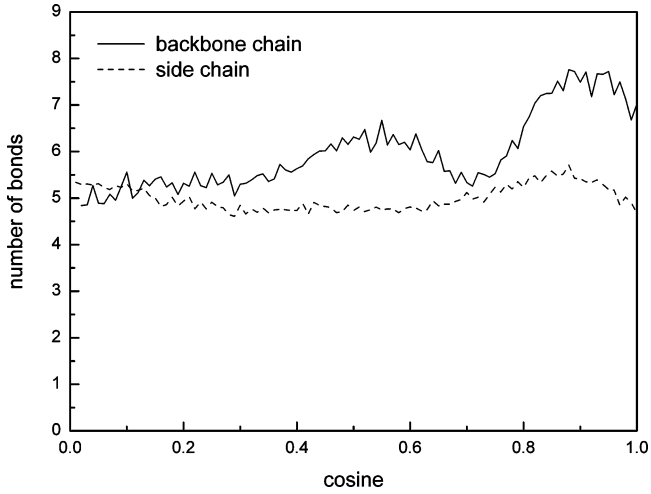

Figure 5. Distribution of the direction cosines of the C−C bonds in the PS backbone and side chain in the direction of stretching (||). The simulations have been carried out at a temperature of 350 K and a pressure of 101.3 kPa. The stretching ratio r_s amounts to 15%.

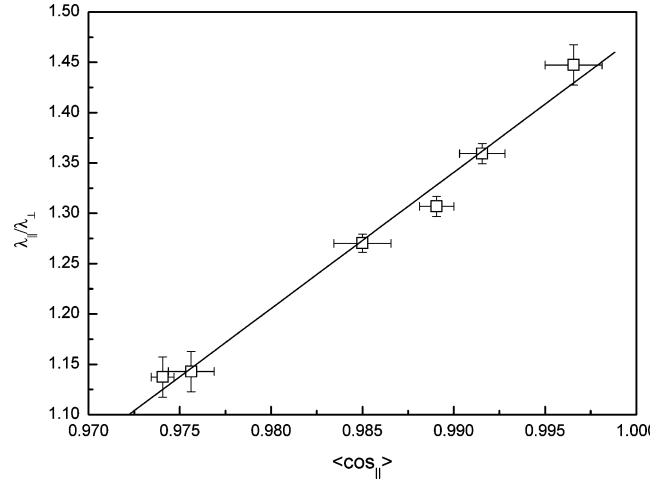

Figure 6. Anisotropy of the thermal conductivity $\lambda_{\parallel}/\lambda_{\perp}$ of PS as a function of the averaged direction cosine of the C−C backbone bonds in the parallel direction $\langle\cos_{\parallel}\rangle$. The RNEMD data have been derived for different temperatures and stretching ratios.

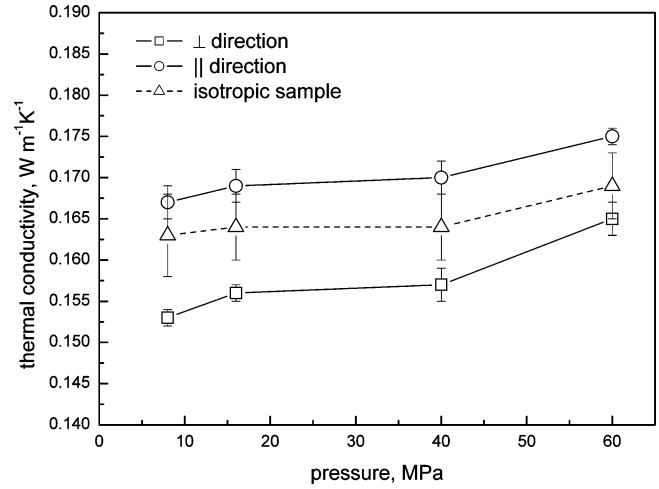

Figure 7. Pressure dependence of the thermal conductivity of a binary PS−CO_2 mixture with 10 mass % of CO_2 and a stretching ratio 22%. The dashed curve for the isotropic mixture has been taken from ref 28.

recognizes that the number of backbone bonds parallel to the stretching direction (cosine ≈ 1) exceeds the number of bonds in the perpendicular direction (cosine ≈ 0).

The parallel profile in Figure 5 exhibits the strongest maximum for a direction cosine of roughly 0.9, indicating that many C−C backbone bonds are oriented almost in the direction of stretching. Since each of the PS backbone carbons lies at the center of a tetrahedron, the angle between the backbone C−C bonds amounts to 109.5°. Thus, the second smaller maximum at about 0.5 follows from this fact. The dashed curve in Figure 5 represents the distribution of the direction cosine of the C−C bonds in the side chain of the polymer. As one can see, there is no preferred orientation of the C−C bonds in this PS unit. This, however, means that the bond orientation in the side chain does not affect the anisotropy of the thermal conductivity. With the data of Figure 5, we have calculated the mean value of the direction cosine of the C−C backbone bonds parallel to the stretching direction. The thermal conductivities perpendicular and parallel to the stretching direction have been calculated as well. The ratio of the thermal conductivities $\lambda_{\parallel}/\lambda_{\perp}$ versus the averaged direction cosine $\langle\cos_{\parallel}\rangle$ is presented in Figure 6. In order to have cosine values between 0 and 1, the data have been scaled. The simulation results have been sampled over a number of temperatures and stretching ratios.

The suggested correlation between the thermal conductivity and the orientation of the C−C backbone bonds is easy to identify in the diagram. The enhancement in the anisotropy of PS with increasing stretching is also a message that follows from the calculated data. Stretching causes an enhanced orientation of the bonds in the PS backbone. This ordering is then responsible for higher $\lambda_{\parallel}$ values. An additional justification of the present correlation can be also deduced from a previous RNEMD simulations of the δ phase of syndiotactic PS.[27] Here, it has been demonstrated that the phenyl rings of PS are more or less irrelevant for the heat transport. Suppression of these degrees of freedom in a simulation does not affect the calculated λ values. Later, we will come back to this point.

3.2. Thermal Conductivity of Mixtures of Stretched Polystyrene and Supercritical Carbon Dioxide. The pressure dependence of the thermal conductivity of a stretched ($r_s = 22\%$) binary mixture with 10 mass % of CO_2 is presented in Figure 7. We have included the data for an isotropic PS−CO_2 mixture from ref 28 (dashed line). Similar to neat PS, the thermal conductivity of the binary mixture is higher in the stretching direction and lower perpendicular to it.

The anisotropy of the thermal conductivity persists at all pressures; however, it is slightly reduced at higher pressure. The thermal conductivities in the parallel and perpendicular directions follow the trend of the thermal conductivity in the isotropic sample;[28] λ is enhanced with increasing pressure. The anisotropy of the thermal conductivity in the binary mixture is much smaller (∼7% difference between $\lambda_{\parallel}$ and $\lambda_{\perp}$) than that in neat PS (∼20%). The CO_2 molecules in the binary mixture introduce additional channels for the heat transfer via collisions[22,23] that do not depend on the anisotropy and thus on the stretching of the polystyrene sample.

The thermal conductivity of binary mixtures as a function of the CO_2 concentration is shown in Figure 8. In analogy to Figure 7, we have added the modification of λ as a function of the CO_2 concentration in the isotropic sample to the diagram. Both the thermal conductivity components $\lambda_{\perp}$, $\lambda_{\parallel}$ and the anisotropy $\lambda_{\parallel}/\lambda_{\perp}$ are reduced with enhanced CO_2 concentration. This reduction of the anisotropy is simple to explain; see again the discussion in connection with Figure 7. With enhanced CO_2 admixtures, the "anisotropic" PS contribution to the thermal

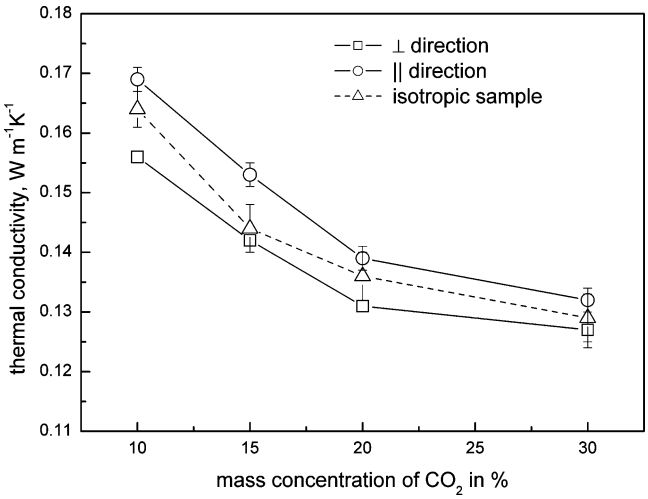

Figure 8. Thermal conductivity of binary PS−CO_2 mixtures as a function of the CO_2 mass concentration at 400 K and 16 MPa for a stretching ratio of 23%. The dashed curve for the isotopic sample has been taken from ref 28.

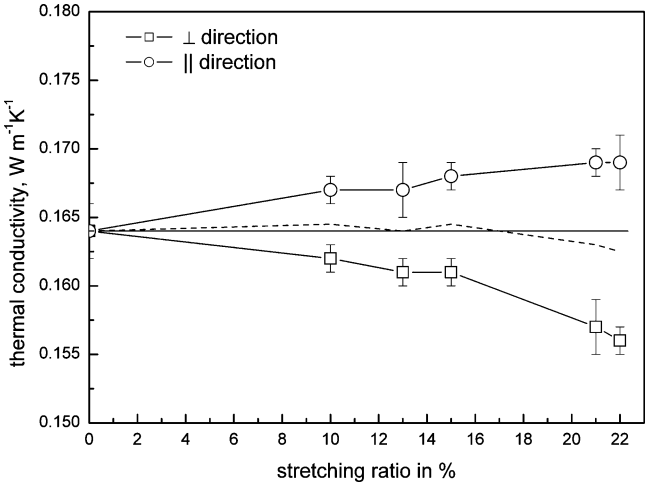

Figure 9. Thermal conductivity of a binary mixture with 10 mass % of CO_2 as a function of the stretching ratio at 400 K and 16 MPa. The mean thermal conductivity $(\lambda_{\|} + \lambda_{\perp})/2$ has been symbolized by a dashed curve. The straight line refers to the thermal conductivity of the isotropic sample which has been taken from ref 28.

conductivity is attenuated while the more or less "isotropic" CO_2 contribution to λ becomes more important.

In Figure 9, we have plotted the thermal conductivity of a binary mixture with 10 mass % of CO_2 as a function of the stretching ratio r_s. The enhancement in the anisotropy of λ with increasing r_s follows a priori expectations. Nevertheless, it is much smaller than that in the neat PS sample. This behavior has been expected, too. Contrary to neat PS, we see that the average of the two curves coincides roughly with the thermal conductivity of the isotropic polymer. Only for large r_s numbers, the mean value of λ in the binary sample is smaller than λ of neat PS. In consideration of the computational error bars, however, we are left with some uncertainties.

Next, let us comment on the correlation between the $\lambda_{\|}/\lambda_{\perp}$ ratio and the average direction cosine $\langle \cos_{\|} \rangle$ for the binary mixtures. For neat PS, this dependence has been displayed in Figure 6. The extension of this diagram to binary systems has been portrayed in Figure 10. In contrast to neat PS, the correlation between the conductivity anisotropy and the average cosine is now less pronounced. Again, we notice that an increasing participation of CO_2 in the heat transport causes an

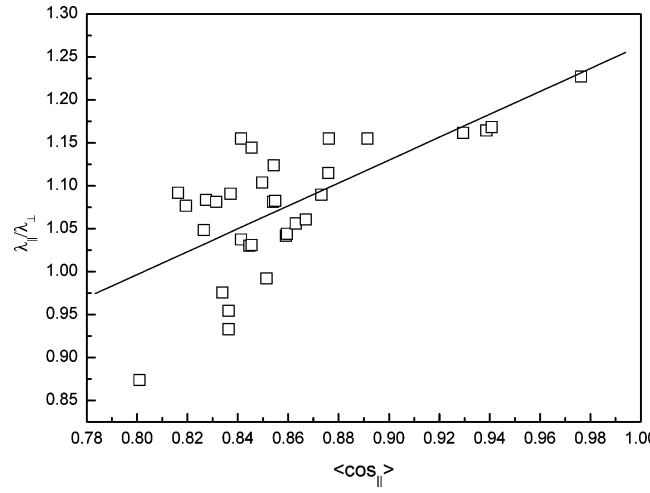

Figure 10. Thermal conductivity ratio $\lambda_{\|}/\lambda_{\perp}$ as a function of the average cosine between the C−C bonds of the backbone and the direction of heat transfer $\langle \cos_{\|} \rangle$ for binary mixtures at different pressures, temperatures, and concentrations of CO_2; see the same correlation for neat PS in Figure 6.

attenuation of the "anisotropic" C−C backbone contribution to the overall conductivity. To reemphasize, the heat transfer contributed by CO_2 occurs via collisions, while the PS participation is phonon driven.

Now, let us consider the dependence of the thermal conductivity on the number of degrees of freedom of the system per unit volume. In our recent research, we have found polymer systems where all vibrational degrees of freedom contribute with the same amount to the thermal conductivity.[12] However, there are a number of factors violating this principle; the most important ones are summarized below. Even in classical MD simulations, we can have a discrimination between strongly localized and delocalized vibrations.[22,23] The latter contribute more efficiently to the transfer of energy than local modes. It is self-explanatory that such a transition between these two boundaries can be tuned artificially by the force-field parameters in a simulation. The importance of the different modes for the thermal conductivity can be quantified by using different patterns of bond constraints and unconstrained geometrical parameters. A convincing argument for the nonequivalence of the degrees of freedom finally follows from the present computational findings, that is, the strong correlation between the orientation of the C−C backbone bonds and λ in PS and PS−CO_2 mixtures. In Figure 11, we have collected calculated thermal conductivities of several materials as a function of the degrees of freedom per unit volume. Changes in the number of degrees of freedom per volume are caused not only by density and concentration variations but also by the use of a force-field with different constraints.

The strong correlation between the number in the degrees of freedom and the thermal conductivity of CO_2 follows from a heat conduction provided via collisions.[22,23] The rather localized vibrations in amorphous materials such as CO_2 without covalent bonding network covering the sample dimension make the heat transfer via phonons highly inefficient.[22,23] In PS, such an extended network is formed by the C−C backbone bonds. The implications for the thermal conductivity have been mentioned above. To come back to the CO_2 data in Figure 11; the higher the density, the more degrees of freedom per unit volume are found and the higher is the collision-driven thermal conductivity.

The thermal conductivities of polyethylene, benzene, and crystalline syndiotactic polystyrene have been taken from

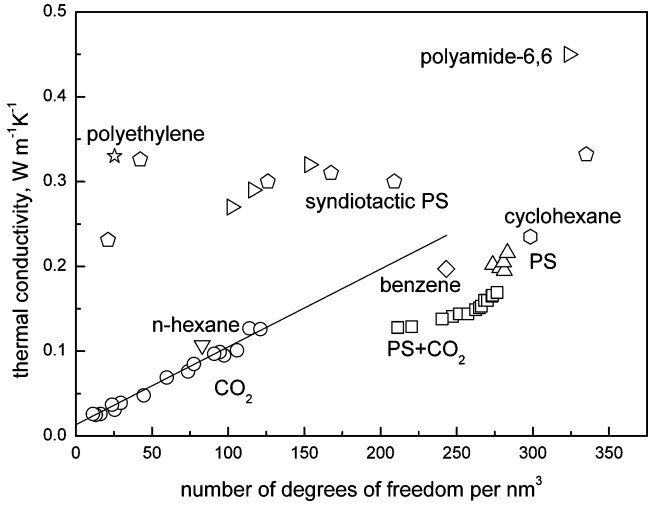

Figure 11. Calculated thermal conductivity as a function of the degrees of freedom per volume for amorphous polyethylene,[47] amorphous polyamide-6,6,[12] crystalline syndiotactic polystyrene,[27] liquid benzene,[26] liquid *n*-hexane,[26] liquid cyclohexane,[26] supercritical CO_2,[28] amorphous atactic polystyrene (present work), and amorphous atactic polystyrene + CO_2 (present work).

previous simulation studies.[26,27,47] The data for amorphous polyethylene are based on a united-atom approach,[47] where one carbon and two hydrogen atoms have been connected to one bead. This step explains the coincidence of a very small number in the degrees of freedom per unit volume and a high thermal conductivity. Responsible for the heat transport in polyethylene are the C−C bonds with their delocalized vibrations, so-called propagons.[23] In analogy to PS, they are a prerequisite to have a highly efficient phonon support in the heat transfer. A second instructive example in Figure 11 is the benzene system, which was modeled using bond constraints throughout. As in CO_2, the heat transport in this hydrocarbon is caused by collisions of the molecules, not by phonons.[22,23] It seems that the thermal conductivity of benzene, *n*-hexane, and cyclohexane can be approximately estimated when extrapolating the CO_2 data to the number of degrees of freedom encountered in these hydrocarbon systems.

The thermal conductivity data for crystalline syndiotactic polystyrene[27] in Figure 11 are highly instructive. The RNEMD calculations in ref 27 have been performed with differences in the degrees of freedom considered, that is, with 0, 8, 6, 11, 15, or 16 constrained bonds per monomer (for more details, see ref 27). In all simulations, except for the completely constrained monomer, the λ values occur around 0.30 W m^{1-} K^{-1}. This, however, means that even a complete suppression of the bond vibrations in the phenyl rings of PS does not influence the thermal conductivity significantly. Only when C−C bonds in the backbone are constrained, the thermal conductivity is strongly reduced. In contrast to syndiotactic polystyrene, the thermal conductivity of amorphous polyamide-6,6 depends strongly and linearly on the number of degrees of freedom per unit volume.[12] Therefore, it seems that the degrees of freedom in polyamide-6,6 are equivalent regarding thermal transport while they are not in polystyrene.

To sum up, the calculated conductivities in Figure 11 indicate quite generally that the collision induced heat transfer is less efficient than the phonon-assisted transfer via long chains with covalent nearest neighbor contacts. From the data in Figure 11, it also follows that this grading between phonon and collision assisted heat transfer is changed in the absence of delocalized modes.

4. Conclusions

The thermal conductivity of stretched PS and PS−CO_2 mixtures has been calculated in a wide pressure, temperature, and concentration range. In neat PS, stretching causes an increase of the thermal conductivity $\lambda_{\|}$ in the stretching direction by up to 20% with a concomitant decrease of the perpendicular thermal conductivity. In the PS−CO_2 mixtures studied here, the anisotropy of the thermal conductivity is reduced (7% higher in the stretching direction) because of an enhanced contribution of the fluid CO_2 which is isotropic. We have found that the orientation of the C−C bonds in the backbone chain relative to the temperature gradient is of great importance. A consequence of the dominance of heat transport through the backbone by phonons is a nonequivalence of the degrees of freedom for the heat transport in PS. In a previous RNEMD simulation,[27] it has been shown that a reduction in the number of degrees of freedom of PS does not affect the thermal conductivity too much. It is however necessary that the suppressed degrees of freedom do not belong to the backbone. The present data are in line with these observations. The stretching of PS has been an efficient tool to study the correlation between the thermal conductivity and the number and orientation of C−C backbone bonds. For pure PS, a simple linear relation has been found between the thermal conductivity anisotropy and the average number of backbone bonds oriented in the direction of the heat transport.

Acknowledgment. We are grateful to the Deutsche Forschungsgemeinschaft for financial support.

References and Notes

(1) Cha, H. J.; Hedrick, J.; DiPietro, R. A.; Blume, T.; Beyers, R.; Yoon, D. Y. *Appl. Phys. Lett.* **1996**, *68*, 1930.
(2) Burrows, P. E.; Gu, G.; Bulovic, V.; Shen, Z.; Forrest, S. R.; Thompson, M. E. *IEEE Trans. Electron Devices* **1997**, *44*, 1188.
(3) Gupta, V. B. *Kolloid Z. Z. Polym.* **1973**, *251*, 117.
(4) Zhang, X. M.; Ajji, A. *J. Appl. Polym. Sci.* **2003**, *89*, 487.
(5) Boika, B. B.; Insarova, N. I.; Lugina, A. S. *Mekhanika Polymerov* **1965**, *1*, 13.
(6) Arns, C. H.; Knackstedt, M. A.; Roberts, A. P.; Pinczewski, V. W. *Macromolecules* **1999**, *32*, 5964.
(7) Washo, B. D.; Hansen, D. *J. Appl. Phys.* **1969**, *40*, 2423.
(8) Morelli, D. T.; Heremans, J.; Sakamoto, M.; Uher, C. *Phys. Rev. Lett.* **1986**, *57*, 869.
(9) Piraux, L.; Kinanyalaoui, M.; Issi, J. P.; Begin, D.; Billaud, D. *Solid State Commun.* **1989**, *70*, 427.
(10) Choy, C. L.; Wong, Y. W.; Yang, G. W.; Kanamoto, T. *J. Polym. Sci., Polym. Phys.* **1999**, *37*, 3359.
(11) Kurabayashi, K.; Asheghi, M.; Touzelbaev, M.; Goodson, K. E. *J. Microelectromech. S.* **1999**, *8*, 180.
(12) Lussetti, E.; Terao, T.; Müller-Plathe, F. *J. Phys. Chem. B* **2007**, *111*, 11516.
(13) Mar, J. D.; Litovsky, E.; Kleiman, J. *J. Build. Phys.* **2008**, *32*, 9.
(14) Müller-Plathe, F. *J. Chem. Phys.* **1997**, *106*, 6082.
(15) Chang, S. H.; Park, S. C.; Shim, J. J. *J. Supercrit. Fluids* **1998**, *13*, 113.
(16) Cooper, A. I. *J. Mater. Chem.* **2000**, *10*, 207.
(17) Nikitin, L. N.; Gallyamov, M. O.; Vinokur, R. A.; Nikolaev, A. Y.; Said-Galiyev, E. E.; Khokhlov, A. R.; Jespersen, H. T.; Schaumburg, K. *J. Supercrit. Fluids* **2003**, *27*, 131.
(18) Kendall, J. L.; Canelas, D. A.; Young, J. L.; DeSimone, J. M. *Chem. Rev.* **1999**, *99*, 543.
(19) Watkins, J. J.; McCarthy, T. J. *Macromolecules* **1994**, *27*, 4845.
(20) Kojima, J.; Takenaka, M.; Nakayama, Y.; Saeki, S. *J. Chem. Eng. Data* **2009**, *54*, 1585.
(21) Binder, K.; Mognetti, B. M.; Macdowell, L. G.; Oettel, M.; Paul, W.; Virnau, P.; Yelash, L. *Macromol. Symp.* **2009**, *278*, 1.
(22) Orbach, R. *Philos. Mag. B* **1992**, *65*, 289.
(23) Allen, P. B.; Feldman, J. L.; Fabian, J.; Wooten, F. *Philos. Mag. B* **1999**, *79*, 1715.
(24) Pasquino, A. D.; Pilswort, Mn. *J. Polym. Sci., Polym. Lett. Ed.* **1964**, *2*, 253.
(25) Müller-Plathe, F. *Phys. Rev. E* **1999**, *59*, 4894.
(26) Zhang, M. M.; Lussetti, E.; de Souza, L. E. S.; Müller-Plathe, F. *J. Phys. Chem. B* **2005**, *109*, 15060.

(27) Rossinsky, E.; Müller-Plathe, F. *J. Chem. Phys.* **2009**, *130*, 134905.
(28) Algaer, E., Alaghemandi, M., Böhm, M. C., Müller-Plathe, F. *J. Phys. Chem. A* **2009**, in press.
(29) Böhm, M. C.; Elsässer, C.; Fähnle, M.; Brandt, E. H. *Chem. Phys.* **1989**, *130*, 65.
(30) Tarmyshov, K. B.; Müller-Plathe, F. *J. Chem. Inf. Model.* **2005**, *45*, 1943.
(31) Müller-Plathe, F. *Comput. Phys. Commun.* **1993**, *78*, 77.
(32) Wu, G.; Li, B. W. *Phys. Rev. B* 2007, *76*.
(33) Yang, N.; Li, N.; Wang, L.; Li, B. *Phys. Rev. B* 2007, *76*.
(34) Li, B. W.; Wang, J.; Wang, L.; Zhang, G. *Chaos* 2005, *15*.
(35) Shenogin, S.; Bodapati, A.; Keblinski, P.; McGaughey, A. J. H. *J. Appl. Phys.* 2009, *105*.
(36) Alaghemandi, M., Leroy, F., Algaer, E., Böhm, M. C., Müller-Plathe F. *Nanotechnology* **2009**, submitted.
(37) Allen, M. P., Tildesley, D. J. *Computer Simulation of Liquids*; Oxford Science Publisher: Oxford, 1987.
(38) Müller-Plathe, F. *Macromolecules* **1996**, *29*, 4782.
(39) Berendsen, H. J. C.; Postma, J. P. M.; Vangunsteren, W. F.; Dinola, A.; Haak, J. R. *J. Chem. Phys.* **1984**, *81*, 3684.
(40) Brown, D. *The gmq user manual verision 4*; University of Savoie, 2008.
(41) Carwille, L. C. K.; Hoge, H. J. "Thermal conductivity of polystyrene: selected values"; Pioneering Research Division: U.S. Army Natick Laboratories, 1966.
(42) Valavala, P. K.; Odegard, G. M. *Rev. Adv. Mater. Sci.* **2005**, *9*, 34.
(43) Harris, J. G.; Yung, K. H. *J. Phys. Chem.* **1995**, *99*, 12021.
(44) Zhang, Z. G.; Duan, Z. H. *J. Chem. Phys.* **2005**, *122*, 214507.
(45) Wang, W. C. V.; Kramer, E. J.; Sachse, W. H. *J. Polym. Sci., Polym. Phys.* **1982**, *20*, 1371.
(46) Riter, J. R. *J. Chem. Phys.* **1970**, *52*, 5008.
(47) Hu, M.; Shenogin, S.; Keblinski, P. *Appl. Phys. Lett.* 2007, *91*.

JP906447A